

Synthesis and electrochemical properties of tetramethyl ammonium salts of $[(\text{PhO})\text{Ni}(\text{CF}_3)_3]^{2-}$ and $[(7\text{-azaindole})\text{Ni}(\text{CF}_3)_3]^{2-}$

Scott T. Shreiber,[†] Roger E. Cramer,[‡] and David A. Vici^{†*}

[†]Department of Chemistry, Lehigh University, 6 E. Packer Ave., Bethlehem, PA, 18015, United States

[‡]Department of Chemistry, University of Hawaii, 2545 McCarthy Mall, Honolulu, HI, 96822, USA

Email: vici@lehigh.edu

Dedicated to Yulia H. Budnikova in recognition of her scientific contributions to the fields of organic chemistry, electrochemistry, and catalysis

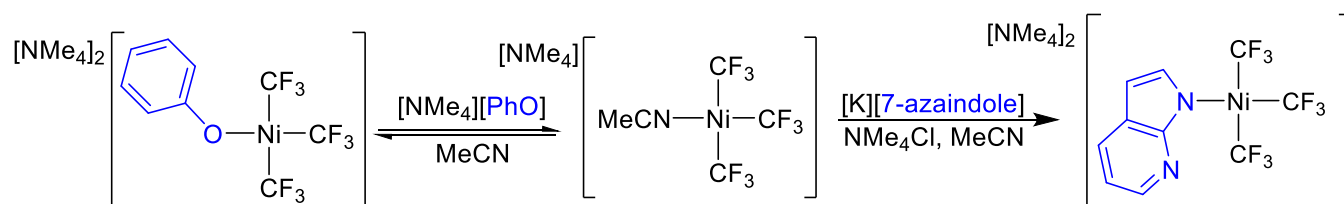
Received 09-12-2022

Accepted Manuscript 10-14-2022

Published on line 10-22-2022

Abstract

The stable tetramethylammonium salts of heteroleptic trifluoromethyl nickelates $[(\text{R})\text{Ni}(\text{CF}_3)_3]^{2-}$ (R = PhO, 7-azaindole) were prepared. The new complexes were characterized by ^1H and ^{19}F NMR spectroscopies and cyclic voltammetry. The phenoxide ligand on $[(\text{PhO})\text{Ni}(\text{CF}_3)_3]^{2-}$ was found to be labile in solution, in contrast to the 7-azaindole ligand on $[(7\text{-azaindole})\text{Ni}(\text{CF}_3)_3]^{2-}$. The electrochemical analysis of the heteroleptic complexes revealed that the dianionic species exhibit oxidations below 0 V vs the Fc/Fc⁺ couple.



simple access to heteroleptic trifluoromethyl nickelate complexes

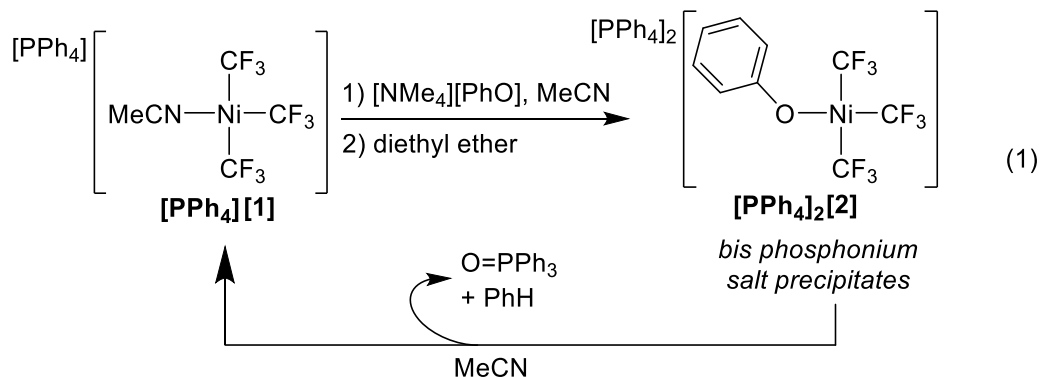
Keywords: Nickel, fluorine, trifluoromethyl, electrochemistry, cyclic voltammetry

Introduction

The introduction of popular fluorinated functionalities such as the trifluoromethyl, difluoromethyl, and monofluorinated groups has proven successful for altering various properties of organic molecules such as acidities, hydrophobicities, conformational biases, and metabolic stabilities.¹⁻⁵ These modifications in turn have rendered molecules that are useful for the pharmaceutical, agrochemical, and materials industries.⁴⁻⁶ Therefore, over the past decade, great interest has been devoted to developing new methodologies for incorporating these simplest of fluorinated functionalities. However, the less common fluorinated functionalities like the $-ZCF_3$ ($Z=O,N$) groups have not received as much attention due to synthetic challenges in their preparation and handling.^{7, 8} This is highlighted by a recent report that showed of the 72 launched drugs up to 2018 that contained the trifluoromethyl group, 69 were connected to carbon, three were connected to oxygen, and none were connected to nitrogen.⁷

A major area of research with the trifluoromethoxy group ($-OCF_3$) has targeted the design of reagents that can transfer OCF_3 to various organic substrates.⁹⁻¹² The trifluoromethoxy group can be sensitive to decomposition, which limits this approach, however some recently developed reagents display surprising stability.¹² Methods for incorporating the trifluoromethylamine ($-NCF_3$) groups has been slower to develop, with many methods requiring the use of harsh chemicals and multi-step synthesis. Only recently has a reagent that can transfer the trifluoromethylamine group to organic substrates has been disclosed.¹³ Therefore, alternative and mild methods to prepare OCF_3 and NCF_3 containing organic molecules remain in-demand.

Our group has been interested in the chemistry of solvated fluoroalkyl nickel complexes for developing new fluoroalkylation reactions. We have shown that $[(MeCN)Ni(R_f)_3]^-$ ($R_f = CF_3, C_2F_5$) can fluoroalkylate a variety of organic electrophiles.^{14, 15} Furthermore, the homoleptic $[Ni(CF_3)_3]^{2-}$ complex can perform catalytic C-H bond trifluoromethylation of (hetero)arenes¹⁵ and catalyze the allylic C-H functionalization of brucine, generating trifluoromethyl neobrucine.¹⁶ Previously, we found that reaction of the phosphonium salt of $[(MeCN)Ni(CF_3)_3]^-$ (**1**) with phenoxide in MeCN followed by precipitation with diethyl ether, leads to the formation of the solid state stable, bis phosphonium salt of $[(PhO)Ni(CF_3)_3]^{2-}$ (**2**) in 80% isolated yield (eq. 1).¹⁴ However, when the bis phosphonium salt of **2** was redissolved in solution, a decomposition reaction to revert back to **1** was observed (eq 1). Therefore, the judicious choice of counter-ion is a critical component in methods developments with these trifluoromethylnickelates. We have now prepared more stable tetramethylammonium salts of **1**¹⁵ as well as derivatives where the acetonitrile was substituted with *N*-heterocyclic carbenes.¹⁷



Therefore, we became interested in revisiting the synthesis of **2** with a tetramethylammonium counter-ion to explore its reaction chemistry in solution. We hypothesized that the increase in anation when converting **1** to **2** would also be accompanied by oxidations that occur at a more negative redox potential that could benefit

methodologies involving oxidatively triggered reductive eliminations of RZ^- ($Z = O, NR$) with CF_3 . Such methodologies for the generation of $RZCF_3$ groups would not rely on the use harsh chemicals limiting substrate scopes or the use of sensitive $-ZCF_3$ reagents, but be more compatible with readily available and commercial substrates.

Results and Discussion

Reaction of the tetramethylammonium salt of **1** with $[NMe_4][OPh]$ in MeCN, followed by precipitation with diethyl ether led to the isolation of the bis-tetramethylammonium salt **2** in 61% isolated yield (eq. 2). The structure was confirmed by X-ray crystallography, and an ORTEP diagram is shown in Figure 1. The structure reveals a distorted square plane around the nickel center, with the CF_3 group trans to the phenoxide as the shortest Ni- CF_3 bond. This feature is consistent with the strong trans influencing properties of the trifluoromethyl ligand. The ^{19}F NMR spectra of the isolated tetramethylammonium salt of **2** at room temperature revealed unique resonances $\delta -21.3$ (sept, 3F) and -31.4 (q, 6F). However, the phenoxide moiety was found to be only weakly coordinated to nickel in solution as the ^{19}F NMR spectrum of **1** in acetonitrile revealed significant quantities of **1**, even at -30 °C (see Supporting Information).

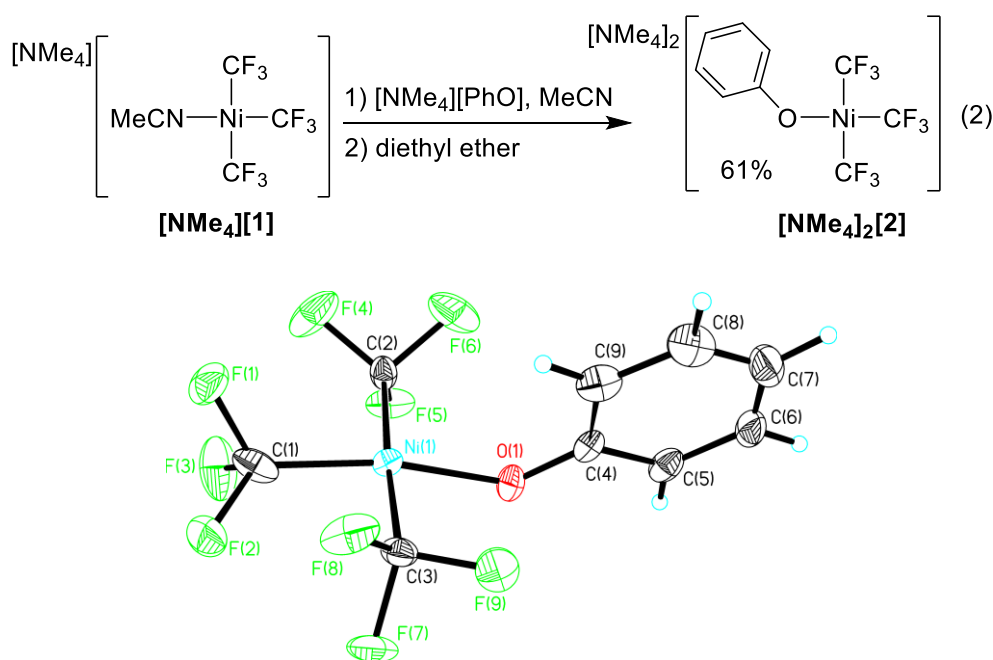
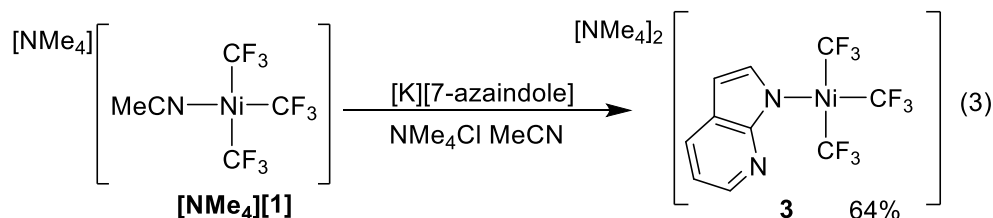


Figure 1. ORTEP Diagram of the anionic portion of **2**. Ellipsoids shown at the 40% level. Selected bond lengths (Å): Ni1-C1 1.876(13); Ni1-O1 1.899(7); Ni1-C3 1.914(12); Ni1-C2 1.920(12). Selected bond angles (°): C1-Ni1-O1 163.0(5); C1-Ni1-C3 92.0(5); O1-Ni1-C3 91.7(4); C1-Ni1-C2 90.8(5); O1-Ni1-C2 87.2(4); C3-Ni1-C2 174.0(5).

Since the phenoxide complex **1** displays a labile Ni-O bond in the presence of acetonitrile, we were curious if nitrogen-bounded X-type ligands displayed similar behavior. Reaction of **1** with deprotonated 7-azaindole led to the formation of the dianionic heterolyptic complex **3** in 64% isolated yield (eq 3). The ^{19}F NMR spectrum revealed diagnostic signals for the new complex $\delta -22.7$ (sept, 3F) and -29.5 (q, 6F). Unlike the phenoxide complex **2**, the 7-azaindole complex **3** was not in equilibrium with **1** in acetonitrile solution, as **1** was not

observed in by NMR spectroscopy, even at room temperature. A preliminary X-ray structure confirms the connectivity of **3** (see Supporting Information), but severe disorders in the structure precludes bond length analyses.



With complexes **2** and **3** in hand, we explored their electrochemical properties by cyclic voltammetry. Tetrabutylammonium hexafluorophosphate was used as the electrolyte to mitigate ion pairing effects of the small tetramethylammonium counter-ions in **2** and **3**. The tetramethylammonium complex of **2** had a first oxidation peak potential at -0.53 V, and a close second oxidation peak potential of -0.36 V vs. the Fc/Fc⁺ couple (Figure 3, blue line). Since it was established that the phenoxide moiety is labile in solution, the cyclic voltammogram of [NMe₄][PhO] was also recorded, and displayed a first oxidation peak potential of -0.40 V (Figure 3, red line). Suggesting that dissociation of phenoxide in solution may lead to the phenoxide moiety itself being oxidized. For comparison, the anionic **1**, has first oxidation peak potential at $+0.38$ V (Figure 3, black line). Overall indicating that phenoxide and/or **2** are more easily oxidized than **1**. However, the dissociation of the phenoxide ligand must be accounted for in future methods developments involving [Ni-OPh] functionalities from trifluoromethylnickelates.

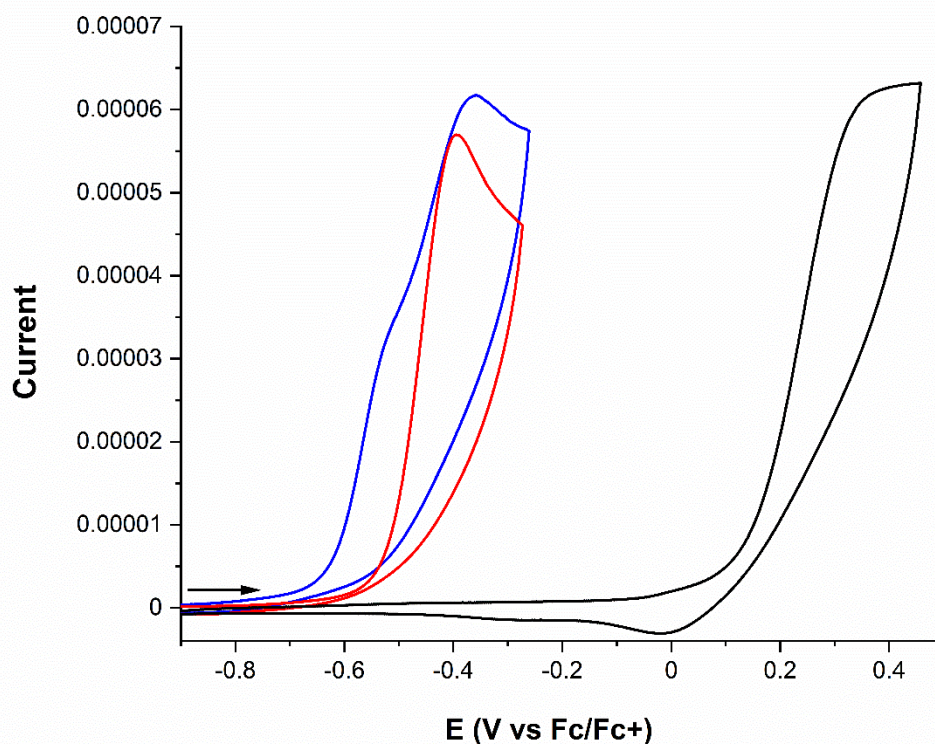


Figure 3. Cyclic voltammogram of [NMe₄]₂[(PhO)Ni(CF₃)₃] (**2**, blue), [NMe₄][PhO] (red), and [NMe₄][(MeCN)Ni(CF₃)₃] (**1**, black) in MeCN. Complex, 10 mM; electrolyte, 100 mM [NBu₄][PF₆]; working and counter electrode, platinum; silver pseudoreference; scan rate 100 mVs⁻¹.

Similarly, the heteroleptic azaindole complex **3** displayed a first oxidation peak potential at -0.13 V vs. the Fc/Fc^+ couple (Figure 4, blue line). Complex **3** also contained other well-separated oxidation peaks at $+0.27$ V and $+0.61$ V (see SI). While complex **3** did not display lability of the coordinated 7-azaindole species, we were curious where the $[\text{K}][7\text{-azaindole}]$ itself underwent oxidative reactivities. The $[\text{K}][7\text{-azaindole}]$ displayed an oxidation peak potential at -0.15 V (Figure 4, red line), in a region similar to the dianionic complex **3**. Again, these oxidation events are far less positive than the anionic solvato complex **1** (Figure 4, black line). Therefore, while the complex **3** has easily accessible oxidation potentials, the polar bond of the 7-azaindole ligand makes it difficult to ascertain if the oxidations involve metal complex or free ligand. The irreversibility of the waves is likely associated with an overall chemical event. Prior investigations with $[(\text{MeCN})\text{Ni}(\text{CF}_3)_3]^-$ and $[(\text{MeCN})\text{Ni}(\text{C}_2\text{F}_5)_3]^-$ suggest that upon oxidation of the nickel complexes in acetonitrile solvent, trifluoromethyl and perfluoroethyl radicals are released, and the charge neutral $[(\text{MeCN})_2\text{Ni}(\text{R}_f)_2]$ is generated.¹⁴⁻¹⁶ This charge-neutral complex in turn gets oxidized at more positive potentials.¹⁴⁻¹⁶ We propose that, when scanning out to more positive potentials during the electrooxidation of **3** (Figure S8, Supporting Information) in acetonitrile solvent, both azaindole radical and CF_3 radical are produced along with the transient formation of $[(\text{MeCN})_2\text{Ni}(\text{CF}_3)_2]$.

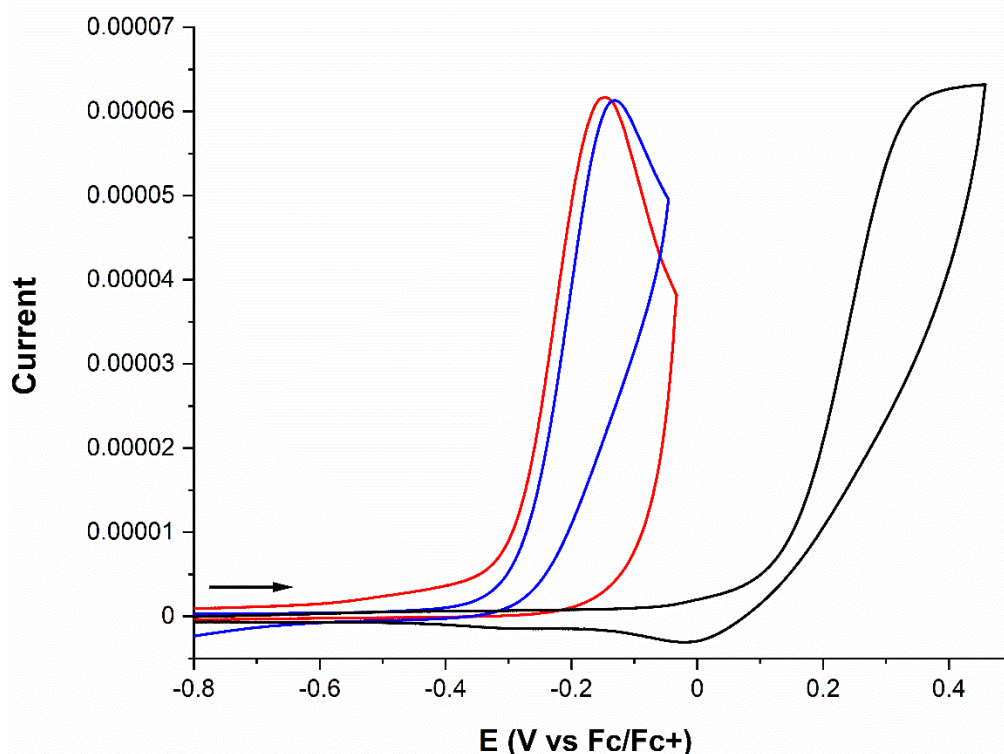


Figure 4. Cyclic voltammogram of $[\text{NMe}_4]_2[(7\text{-azaindole})\text{Ni}(\text{CF}_3)_3]$ (**3**, blue), $[\text{k}][7\text{-azaindole}]$ (red), and $[\text{NMe}_4][(\text{MeCN})\text{Ni}(\text{CF}_3)_3]$ (**1**, black) in MeCN. Complex, 10 mM; electrolyte, 100 mM $[\text{NBu}_4][\text{PF}_6]$; working and counter electrode, platinum; silver pseudoreference; scan rate 100 mVs^{-1} .

Conclusions

In this report, we have disclosed the synthesis of stable tetramethylammonium salts of heteroleptic trifluoromethyl nickelate salts $[\text{RNi}(\text{CF}_3)_3]^{2-}$ ($\text{R} = \text{PhO}$, 7-azaindole). While the phenoxide in $[(\text{PhO})\text{Ni}(\text{CF}_3)_3]^{2-}$ could be displaced by acetonitrile to form $[(\text{MeCN})\text{Ni}(\text{CF}_3)_3]^-$, the azaindole anion in $[(\text{azaindole})\text{Ni}(\text{CF}_3)_3]^{2-}$ was more tightly bound to the nickel and did not revert to $[(\text{MeCN})\text{Ni}(\text{CF}_3)_3]^-$ upon dissolution in acetonitrile. Full characterization of the new nickel complexes is reported, and their electrochemical properties are revealed. Both the phenoxide and azaindole nickel complexes display irreversible oxidations at potentials near the values for free phenoxide and free azaindole, suggesting that oxidative chemistries involving these nickel complexes may ultimately involve free phenoxide and azaindole radicals.

Experimental Section

General Considerations: All manipulations were performed using standard Schlenk and high vacuum techniques or in a nitrogen filled glovebox, unless otherwise stated. Solvents were purified by passing through activated alumina and/or copper in a solvent purification system supplied by Pure Process Technology. Solution ^1H NMR spectra were recorded at ambient temperature on a Bruker 400 MHz spectrometer and referenced to residual proton solvent signals. ^{19}F NMR spectra were recorded on the Bruker NMR spectrometer operating at 376 MHz and referenced to α,α,α -trifluorotoluene as an internal standard ($\delta = -63.7$). A Bruker D8 Quest diffractometer was used for X-ray crystal structure determinations. Cyclic voltammetry data was collected in a nitrogen filled glovebox at room temperature on a PARSTAT 4000A potentiostat. CCDC 2195893 and 2203186 contain the supplementary crystallographic data for compounds **2** and **3** in this paper, respectively. These data can be obtained free of charge via www.ccdc.cam.ac.uk/data_request/cif, or by e-mailing data_request@ccdc.cam.ac.uk, or by contacting The Cambridge Crystallographic Data Centre, 12 Union Road, Cambridge CB2 1EZ, UK; fax: +44 1223 336033.

Preparation of $[\text{NMe}_4]_2[(\text{PhO})\text{Ni}(\text{CF}_3)_3]$ (2**):** In a glovebox, a solution of $[\text{NMe}_4][\text{OPh}]$ (13 mg, 0.08 mmol) in 0.5 mL of MeCN was added to a stirred solution of $[\text{NMe}_4][(\text{MeCN})\text{Ni}(\text{CF}_3)_3]$ (30 mg, 0.08 mmol) in 0.5 mL of MeCN. The solution was stirred for 30 minutes, and then 1 mL of ether was added. The vial was placed in the glovebox freezer ($-30\text{ }^\circ\text{C}$) where yellow crystals formed and were collected (25 mg, 61%). The solution ^1H NMR spectra were complicated due to the lability of the phenoxide ion resulting in the equilibria observed between the phenoxide complex **2** and **1**. ^{19}F NMR (CD_3CN , 376 MHz): δ -21.3 (sept, $J = 4.1$ Hz, 3F), -31.4 (q, $J = 4.1$ Hz, 6F). Anal. Calcd (found) for $\text{C}_{17}\text{H}_{29}\text{NiF}_9\text{N}_2\text{O}$: C, 40.26 (40.59); H, 5.76 (5.48).

Preparation of $[\text{NMe}_4]_2[(7\text{-azaindole})\text{Ni}(\text{CF}_3)_3]$ (3**):** In a glovebox, to a stirred solution of $[\text{NMe}_4][(\text{MeCN})\text{Ni}(\text{CF}_3)_3]$ (38 mg, 0.10 mmol) and NMe_4Cl (12 mg, 0.10 mmol) in 0.5 mL of MeCN was added a solution of $[\text{K}][7\text{-azaindole}]$ (16 mg, 0.10 mmol) in 1.5 mL of MeCN, and then the resulting mixture was stirred for 15 minutes. The insolubles were removed by filtration, and ether was added to the solution to precipitate the product. After placing in the glovebox freezer ($-30\text{ }^\circ\text{C}$) overnight, the product was collected by filtration and washed with ether to yield 34 mg (64%) of a light yellow solid. ^1H NMR (CD_3CN , 376 MHz): δ 8.04 (dd, $J = 4.6$ Hz, 1.8 Hz, 1H), 7.53 (dd, $J = 7.5$ Hz, 1.8 Hz, 1H), 7.42 (d, $J = 2.7$ Hz, 1H), 6.58 (dd, $J = 7.5$ Hz, 4.6 Hz, 1H), 6.08 (d, $J = 2.7$ Hz, 1H), 3.12 (s, 12H). ^{19}F NMR (CD_3CN , 376 MHz): δ -22.7 (sept, $J = 4.1$ Hz, 3F), -29.5 (q, $J = 4.1$ Hz, 6F). Anal. Calcd (found) for $\text{C}_{18}\text{H}_{29}\text{NiF}_9\text{N}_4$: C, 40.70 (41.42); H, 5.50 (5.90).

Acknowledgements

D.A.V. thanks the U.S. National Science Foundation (CHE-2153730) for support of this work.

Supplementary Material

The supporting spectral data are provided in the Supplementary Material file associated with this manuscript.

References

1. Ni, C.; Hu, J., *Chem. Rev.* **2016**, *45*, 5441-5454.
<https://doi.org/10.1039/C6CS00351F>
2. Purser, S.; Moore, P. R.; Swallow, S.; Gouverneur, V., *Chem. Soc. Rev.* **2008**, *37*, 320-330.
<https://doi.org/10.1039/B610213C>
3. Wang, J.; Sánchez-Roselló, M.; Aceña, J. L.; del Pozo, C.; Sorochinsky, A. E.; Fustero, S.; Soloshonok, V. A.; Liu, H., *Chem. Rev.* **2014**, *114*, 2432-2506.
<https://doi.org/10.1021/cr4002879>
4. Ogawa, Y.; Tokunaga, E.; Kobayashi, O.; Hirai, K.; Shibata, N., *iScience* **2020**, *23*, 101467.
<https://doi.org/10.1016/j.isci.2020.101467>
5. Inoue, M.; Sumii, Y.; Shibata, N., *ACS Omega* **2020**, *5* (19), 10633-10640.
<https://doi.org/10.1021/acsomega.0c00830>
6. Fang, Z.; Peng, Y.; Zhou, X.; Zhu, L.; Wang, Y.; Dong, X.; Xia, Y., *ACS Applied Energy Materials* **2022**, *5*, 3966-3978.
<https://doi.org/10.1021/acsaem.1c03476>
7. Schiesser, S.; Chepliaka, H.; Kollback, J.; Quennesson, T.; Czechtizky, W.; Cox, R. J., *J. Med. Chem.* **2020**, *63*, 13076-13089.
<https://doi.org/10.1021/acs.jmedchem.0c01457>
8. Feng, P.; Lee, K. N.; Lee, J. W.; Zhan, C.; Ngai, M.-Y., *Chem. Sci.* **2016**, *7*, 424-429.
<https://doi.org/10.1039/C5SC02983J>
9. Zheng, W.; Lee, J. W.; Morales-Rivera, C. A.; Liu, P.; Ngai, M.-Y., *Angew. Chem. Int. Ed.* **2018**, *57*, 13795-13799.
<https://doi.org/10.1002/anie.201808495>
10. Zhou, M.; Ni, C.; Zeng, Y.; Hu, J., *J. Am. Chem. Soc.* **2018**, *140*, 6801-6805.
<https://doi.org/10.1021/jacs.8b04000>
11. Newton, J. J.; Jelier, B. J.; Meanwell, M.; Martin, R. E.; Britton, R.; Friesen, C. M., *Org. Lett.* **2020**, *22*, 1785-1790.
<https://doi.org/10.1021/acs.orglett.0c00099>
12. Lee, K. N.; Lee, J. W.; Ngai, M.-Y., *Tetrahedron* **2018**, *74*, 7127-7135.
<https://doi.org/10.1016/j.tet.2018.09.020>
13. Liu, S.; Huang, Y.; Wang, J.; Qing, F.-L.; Xu, X.-H., *J. Am. Chem. Soc.* **2022**, *144*, 1962-1970.
<https://doi.org/10.1021/jacs.1c12467>

14. Shreiber, S. T.; DiMucci, I. M.; Khrizanforov, M. N.; Titus, C. J.; Nordlund, D.; Dudkina, Y.; Cramer, R. E.; Budnikova, Y.; Lancaster, K. M.; Vivic, D. A., *Inorg. Chem.* **2020**, *59*, 9143-9151.
<https://doi.org/10.1021/acs.inorgchem.0c01020>
15. Shreiber, S. T.; Vivic, D. A., *Angew. Chem. Int. Ed.* **2021**, *60*, 18162-18167.
<https://doi.org/10.1002/anie.202104559>
16. Shreiber, S. T.; Puchall, G. I.; Vivic, D. A., *Tetrahedron Lett.* **2022**, 153795.
<https://doi.org/10.1016/j.tetlet.2022.153795>
17. Shreiber, S. T.; Amin, F.; Schäfer, S. A.; Cramer, R. E.; Klein, A.; Vivic, D. A., *Dalton Trans.* **2022**, *51*, 5515-5523.
<https://doi.org/10.1039/D2DT00511E>

This paper is an open access article distributed under the terms of the Creative Commons Attribution (CC BY) license (<http://creativecommons.org/licenses/by/4.0/>)